

Article

The ferraquinone – ferrahydroquinone couple: combining quinonic and metal-based reactivity

Alexander Dauth, Urs Gellrich, Yael Diskin-Posner, Yehoshoa Ben-David, and David Milstein

J. Am. Chem. Soc., **Just Accepted Manuscript** • DOI: 10.1021/jacs.6b13050 • Publication Date (Web): 31 Jan 2017

Downloaded from <http://pubs.acs.org> on February 3, 2017

Just Accepted

“Just Accepted” manuscripts have been peer-reviewed and accepted for publication. They are posted online prior to technical editing, formatting for publication and author proofing. The American Chemical Society provides “Just Accepted” as a free service to the research community to expedite the dissemination of scientific material as soon as possible after acceptance. “Just Accepted” manuscripts appear in full in PDF format accompanied by an HTML abstract. “Just Accepted” manuscripts have been fully peer reviewed, but should not be considered the official version of record. They are accessible to all readers and citable by the Digital Object Identifier (DOI®). “Just Accepted” is an optional service offered to authors. Therefore, the “Just Accepted” Web site may not include all articles that will be published in the journal. After a manuscript is technically edited and formatted, it will be removed from the “Just Accepted” Web site and published as an ASAP article. Note that technical editing may introduce minor changes to the manuscript text and/or graphics which could affect content, and all legal disclaimers and ethical guidelines that apply to the journal pertain. ACS cannot be held responsible for errors or consequences arising from the use of information contained in these “Just Accepted” manuscripts.

The ferraquinone – ferrahydroquinone couple: combining quinonic and metal-based reactivity

Alexander Dauth^{†, δ} Urs Gellrich^{†, δ} Yael Diskin-Posner,[‡] Yehoshoa Ben-David,[†] David Milstein^{*, †}

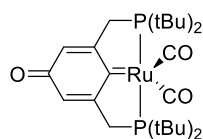
[†]Department of Organic Chemistry and [‡]Department of Chemical Research Support, Weizmann Institute of Science, Rehovot, 76100, Israel

ABSTRACT: A ferraquinone – ferrahydroquinone organometallic redox-couple was prepared and characterized. Intricate cooperativity of the metal is observed with different positions on the ligand. This allowed cooperative activation of small molecules like molecular hydrogen, oxygen and bromine. Likewise, dehydrogenation of alcohols was achieved through 1,6 metal-ligand cooperation.

Introduction

Quinones are prevalent in biological and chemical redox processes.¹ For example, the production of hydrogen peroxide utilizing anthraquinone is performed yearly on a multi-ton scale.² Quinones like DDQ or chloranil are routinely used for oxidation reactions in academic laboratories.^{3–9} Likewise, quinonic cofactors like ubiquinone (coenzyme Q10) play an essential role in the respiratory chain of almost all aerobic organisms and act as antioxidants in the body.^{10,11} Recently, quinones have also found utilization in transdisciplinary applications like enzymatic fuel cells.¹² We sought to combine the redox properties of quinonic compounds with suitable transition metals in the anticipation to observe new cooperative patterns which can in turn lead to novel chemical transformations. To this end we envisaged the employment of iron which has experienced a renaissance in its use in transition metal catalysis due to its obvious ecological and economic benefits.^{13–25}

Scheme 1. The only metallaquinone reported to date.



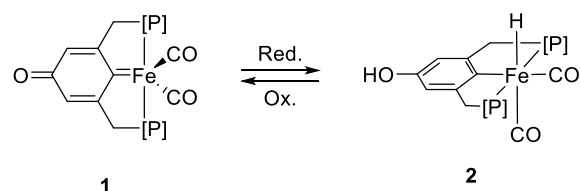
Ruthenaquinone

Several years ago, our group reported the formation of the first and only metallaquinone, in which an oxygen atom of a quinone is replaced by a metal, namely the ruthenaquinone depicted in Scheme 1.²⁶ Spectroscopic and computational studies of this new compound class were performed but no further reactivity studies were undertaken. Specifically, the spectral properties were solvent-dependent, which was ascribed to the presence of an overall quinonic structure in non-polar solvents, while a zwitterionic structure was stabilized in more polar solvents.

Other reports from our group described phenoxonium cations as well as quinone methides stabilized by transition metals.^{27–29} A number of organometallic species are known which contain ortho- and para-quinonic moieties^{30–32} in their ligand framework but in no other case is the metal center an integral part of the quinonic system.^{33–35} Based on our earlier findings²⁶ we intended to prepare a corresponding complex of earth-abundant iron, ferraquinone **1**, with its hydrogenated counterpart – a ferrahydroquinone **2** – and to investigate the

general reactivity of the resulting redox couple towards the activation of small molecules (Scheme 2).

Scheme 2. Envisioned ferraquinone-hydroferraquinone redox couple.



Specifically, the role and mode of metal ligand-cooperation in this system was explored in the various transformations facilitated by the system. In recent years cooperation between the metal and the supporting ligands has led to unprecedented reactivity which harvests both the reactivity of the metal as well as the ligand.^{36–40}

Results and discussion

The phenolic PCP pincer ligand 3,5-bis-(di-isopropylphosphinomethylene)phenol **3** was prepared (see Supplementary Information, SI) and reacted with $\text{Fe}(\text{CO})_5$ in THF under UVB irradiation (Scheme 3). After 4 days, ligand metalation was complete and a highly air sensitive, green crystalline solid was obtained. The product was identified by NMR analysis as ferrahydroquinone-hydride **2** exhibiting a clear triplet in the ¹H NMR spectrum at -8.83 ppm in C_6D_6 characteristic for a hydride cis to two equivalent P ligands and trans to CO as a strong π -acceptor ligand. The ring proton of the pincer ligand was found at 6.48 ppm which is typical for the aromatic protons in organic hydroquinones.

X-ray quality crystals were obtained by slow diffusion of pentane into an ether/pentane solution of **2** (Figure 1).⁴¹ The unusually expansive unit cell (see SI) contains 12 molecules in the asymmetric unit cell of **2** and confirms the formation of the ferrahydroquinone-hydride di-carbonyl complex as a distorted octahedron. The bond distance between the iron center and the ipso carbon of the ligand (C1) is 2.070(4) Å. This is slightly longer than the Fe-C(ipso) distance in the related POCOP iron pincer bis-carbonyl hydride complex reported by Guan et al. (1.995 Å).⁴² In the ligand scaffold, the C5 – O1 bond is 1.440(6) Å, slightly longer than the C–O single bond in organic hydroquinone (1.392 Å). The P1 – Fe – P2 and C1 – Fe – C21 bond angles are smaller than 180° with 159.10(6)° and 170.8(3)° respectively, while the angle between the CO ligands is almost a proper right angle at 88.8(3)°.

Scheme 3. Preparation of 1 and 2.

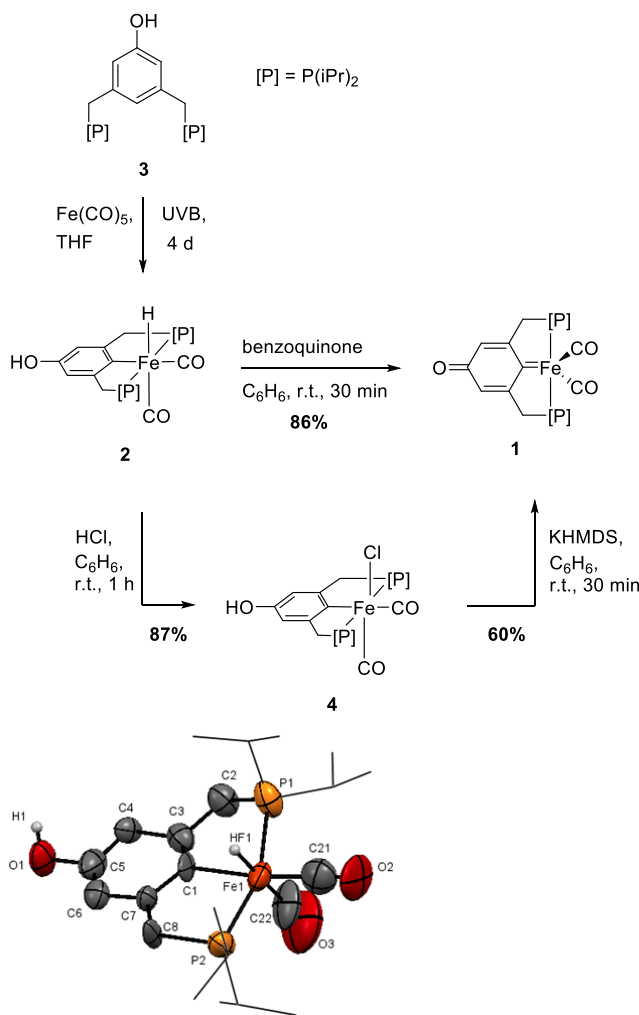


Figure 1. Solid state structure of 2 (thermal ellipsoids set at 50% probability level; isopropyl groups presented as wireframe and hydrogens omitted for clarity). Selected bond lengths [Å] and angles [°] for 2: Fe1 – C21 1.747(8), Fe1 – C22 1.640(6), Fe1 – P1 2.239(2), Fe1 – P2 2.276(2), Fe1 – C1 2.070(4), C5 – O1 1.440(6), C1 – C7 1.394(6), C7 – C6 1.427(6), C6 – C5 1.340(7), P1 – Fe1 – P2 159.10(6), C1 – Fe1 – C21 170.8(3), C1 – Fe1 – C22 99.5(3), C21 – Fe1 – C22 88.8(3). Data collected at ESRF ID-29.⁴³

Ferraquinone-hydride 2 was treated with two equiv. benzoquinone in order to transform it to the ferraquinone 1. High resolution mass spectrometry confirmed the formal loss of H₂ by the dehydrogenation of 2 with benzoquinone. Further support for the formation of a quinonic structure comes from NMR data which show the signal of the ring-proton in the phenyl moiety of the pincer ligand at 6.87 ppm which is also typical for organic quinones. Likewise, the carbonyl-carbon gives a signal at 170 ppm in the ¹³C NMR, slightly up-field from organic quinones. The carbenoid *ipso*-carbon could not be detected, possibly due to fast relaxation through the neighboring Fe center or due to trace paramagnetic impurities.⁴⁴ As X-ray quality crystals could not be obtained, ferraquinone 1

was also prepared independently *via* a two-step sequence in order to confirm its formation (Scheme 3). In a first step, a benzene solution of 2 was treated with aqueous hydrochloric acid. The corresponding ferraquinone chloride complex 4 was formed as a light yellow solid in 87% yield. The ¹H NMR spectrum of 4 confirmed the elimination of the hydride ligand and the solid-state structure also showed the replacement of the hydride by a chloride ligand (Figure 2).

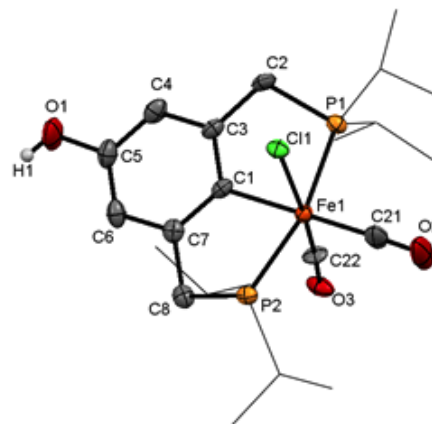


Figure 2. Solid state structure of 4 (thermal ellipsoids set at 50% probability level; isopropyl groups presented as wireframe and hydrogens omitted for clarity). Selected bond lengths [Å] and angles [°] for 4: Fe1 – C21 1.801(5), Fe1 – C22 1.660(1), Fe1 – C11 2.402(3), Fe1 – C1 2.041(4), Fe1 – P1 2.265(2), Fe1 – P2 2.274(2), C5 – O1 1.381(6), C1 – C7 1.402(8), C6 – C7 1.400(7), C5 – C6 1.384(8), P1 – Fe1 – P2 165.14(5), C1 – Fe1 – C21 179.6(4), C1 – Fe1 – C11 87.5(2), C21 – Fe1 – C22 93.6(4).

Again, the complex adopts a slightly distorted octahedral geometry with the Fe1 – C1 bond length being 2.041(4) Å and the Fe1 – C11 distance 2.402(3) Å. The ligand is aromatic with C – C bond lengths varying slightly between 1.384 and 1.403 Å and the C – O bond being a typical hydroquinonic single bond at 1.381(6) Å. Consequently, the phenolic position of complex 4 was deprotonated with KHMDS in benzene which led to formation of ferraquinone 1 in 60% yield with identical spectral properties as after reaction of 2 with benzoquinone. In contrast to the previously reported ruthenaquinone,²⁶ the spectral properties of 1 were not dependent on the polarity of the solvent and it was found soluble in a wide spectrum of organic solvents ranging from methanol, acetonitrile, tetrahydrofuran and dichloromethane to diethyl ether and pentane. The addition of external ligands like CO, acetonitrile or PPh₃ did not affect the spectral properties of 1, signifying a coordinative saturated complex. Indeed, calculations at the BP86-D3/def2-TZVP level of theory clearly minimize 1 in a quinonic geometry as a trigonal bipyramid.⁴⁵ The C–O bond in the ligand was calculated to be a double bond at 1.25 Å and the C–C bond lengths in the aryl moiety varied from 1.46 Å for the single bonds to 1.37 Å for the double bonds in conjugation with the quinonic C=O double bond (Figure 3). The angle between the CO ligands is 96° which is corroborated by the FT-IR spectrum of 1 where the CO ligands appear as two bands of almost equal intensity at 1978 and 1919 cm⁻¹. These values are in turn in good agreement with the data reported for the ruthenaquinone system (1983, 1926 cm⁻¹). The quinonic C=O bond stretch falls at relatively low wavenumbers (1563 cm⁻¹) suggesting a strong contribution of the metal center to the electronic structure of the ligand. This observation is qualitatively confirmed by frequency calculations at the BP86-D3/def2-TZVP, rendering this band at 1583 cm⁻¹.

Having established synthetic routes to both members of the ferraquinone–ferrahydroquinone couple, **1** and **2**, we set out to investigate their reactivity with special attention to cooperativity between metal and ligand.

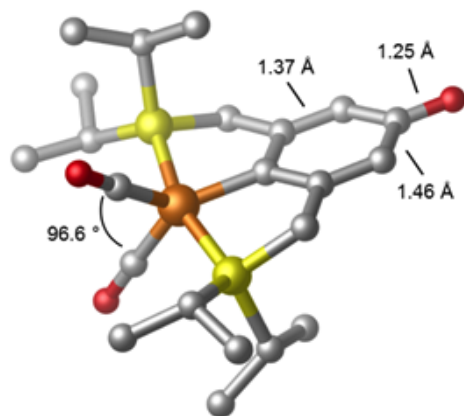
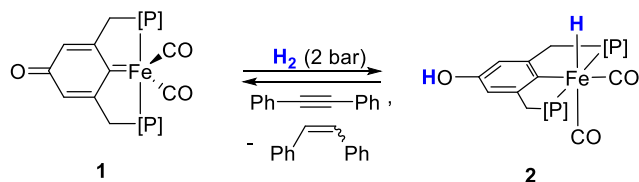


Figure 3. DFT optimized structure of **1** (BP86-D3/def2-TZVP).

Initially, we were interested whether **1** could be directly transformed into **2** by activation of molecular hydrogen. When a solution of **1** in C_6D_6 was pressurized with two bar H_2 , formation of **2** was observed after 18 hours (Scheme 4). Under UVB irradiation, the reaction was complete after only 2 hours.

Scheme 4. Reaction of **1** with H_2 via a formal 1,6-addition.



The mechanism of the thermal hydrogen activation by the ferraquinone **1** was examined by DFT calculations at the SMD(benzene)-TPSS-D3BJ/def2-TZVPP//BP86-D3/def2-SV(P) level of theory (Figure 4). Direct addition of H_2 to the Fe- C_{ipso} is possible according to the calculations via a low barrier of 21.4 kcal/mol. A subsequent keto-enol tautomerization yields the Ferrahydroquinone-hydride **2** in an overall exergonic reaction.

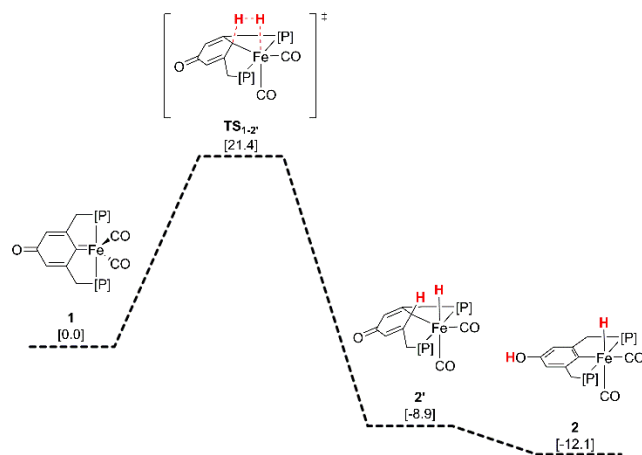
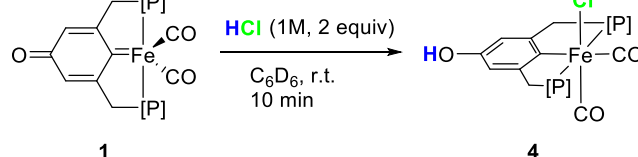


Figure 4. Free energy pathway for the H_2 activation by the ferraquinone **1**, calculated at the TPSS-D3BJ/def2-TZVPP//BP86-D3/def2-SV(P) level of theory. Solvent effects are implicit taken into account by using the SMD model.

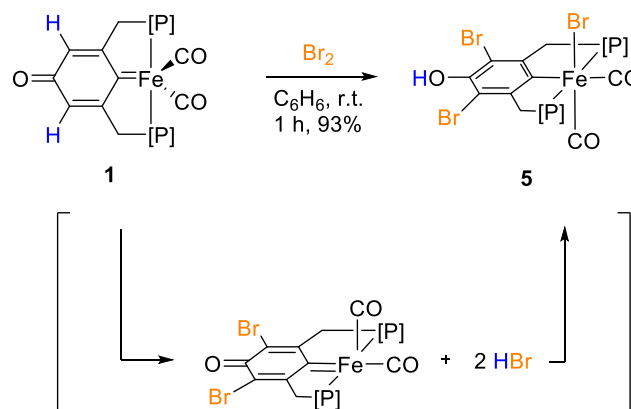
The net-reaction comprises a formal 1,6 type cooperation of the Fe center with the carbonyl oxygen in the para-position of the ligand. Ferrahydroquinone **2** is resistant to acceptorless H_2 loss when heated in boiling toluene. Likewise, heating **2** to $200^\circ C$ as a solid under vacuum left the starting material unchanged.⁴⁶ These findings are in agreement with the calculated ΔG for the H_2 activation (Figure 4). When **2** was reacted with a large excess (at least 10 equivalents) diphenylacetylene as hydrogen acceptor under UVB irradiation, disappearance of **2** and formation of **1** was confirmed by IR spectroscopy. Concomitant formation of a 3:1 mixture of Z and E-stilbene was detected by GCMS. The hydrogen transfer could also be observed with phenylacetylene as substrate, yielding styrene and ethylbenzene in a 15:1 mixture as determined by GC-MS. Treating **1** with dilute mineral acid like HCl yielded the ferrahydroquinone-chloride complex **4** (Scheme 5). As can be seen, the proton was transferred to the para-oxygen on the ligand while the chloride is bound to the metal center.

Scheme 5. Reaction of **1** with HCl via a formal 1,6-addition.



Organic quinones are known to undergo hydrogen-halogen exchange at the ring via halogen (X_2) addition followed by HX elimination.¹² We were interested to see whether a similar behavior could be observed with ferraquinone **1**. Indeed, reaction with 2.2 equivalents of a 1wt% Br_2 benzene solution proceeded rapidly to form a new organometallic species. This compound was identified by NMR, FT-IR, MS and X-ray crystallography to be ferrahydroquinone-bromide **6** with a brominated aryl moiety of the PCP pincer ligand in both meta-positions to the metal (Scheme 6, Figure 5).

Scheme 6. Formation of **5** by treatment of **1** with elemental bromine.



The solid state structure shows a slightly distorted octahedral geometry around the metal center with a Fe1 – C1 bond length of 2.031(4) Å and a Fe1 – Br3 distance of 2.4900(7) Å (Figure 5). In the ring moiety of the pincer ligand C – C bond lengths vary slightly between 1.392 and 1.405 Å and the C – O bond is a single bond at 1.356(4) Å, demonstrating aromaticity of the ring. C – Br bond lengths are essentially equal 1.904(3) and 1.906(4) Å.

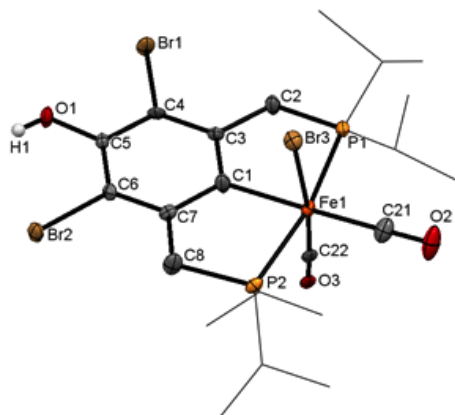
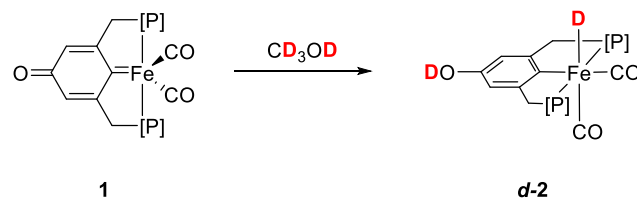
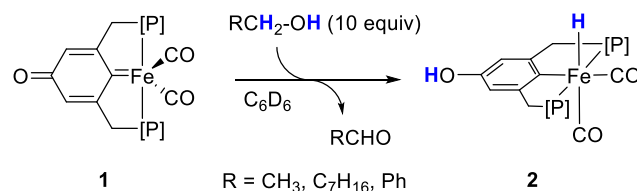


Figure 5. Solid state structure of **5** (thermal ellipsoids set at 50% probability level; isopropyl groups presented as wireframe and hydrogens omitted for clarity). Selected bond lengths [Å] and angles [°] for **5**: Fe1 – C21 1.813(4), Fe1 – C22 1.765(4), Fe1 – Br3 2.4900(7), Fe1 – C1 2.031(4), Fe1 – P1 2.268(1), Fe1 – P2 2.279(1), –C5 – O1 1.356(4), C4 – Br1 1.906(4), C6 – Br2 1.904(3), C1 – C3 1.404(5), C3 – C4 1.392(5), C4 – C5 1.396(5), P1 – Fe1 – P2 168.23(4), C1 – Fe1 – C21 177.3(2), C1 – Fe1 – Br3 89.1(1), C21 – Fe1 – C22 98.5.

A likely mechanism for this transformation is analogous to hydrogen-halogen substitution in organic quinones, namely, Br₂ addition to the quinonic double bonds, followed by HBr elimination. The HBr liberated during this step is immediately incorporated into the complex, akin to the reaction of **1** with HCl (Scheme 6).

Furthermore, it was found that when standing in alcoholic solutions for 18 hours at room temperature, ferraquinone **1** was also quantitatively converted into ferrahydroquinone **2**. The reaction time could be significantly decreased to 2 hours by UVB irradiation. At the same time, formation of the corresponding aldehyde and no other organic products was observed by GCMS. Short and medium chain aliphatic alcohols as well as benzyl alcohol were stoichiometrically dehydrogenated to their corresponding aldehydes (Scheme 7).

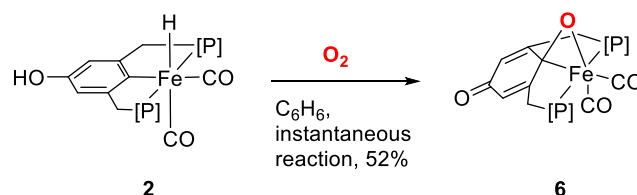
Scheme 7. Dehydrogenation of alcohols mediated by **1**.



Using a deuterated alcohol like CD₃OD afforded **d-2** which was evident from the absence of a hydride signal in the ¹H NMR spectrum while the ³¹P NMR spectrum displayed a 1:1:1 triplet at 110.5 ppm for the coordinated ligand, showing the coupling of the two equivalent phosphorus atoms with a deuteride (Scheme 7). As in the reaction with H₂ and HCl, a formal 1,6-type metal-ligand cooperation is involved in the oxidation of alcohols.

When a THF or benzene solution of **2** was exposed to air, an instantaneous color change to deep orange was observed. X-ray quality crystals were obtained from a cooled toluene solution layered with diethylether and the solid-state structure revealed the formation of oxaferraquinone **6**. One oxygen atom has been incorporated into the complex and is bridging the metal center and the pincer ligand in a 1,2 fashion in the *ipso* position (Scheme 8).

Scheme 8. Formation of the oxaferraquinone **6** by exposure of **2** to oxygen.



The solid state bond lengths as well as computational analysis (NBO, Mayer bond order and bond critical point analyses)⁴⁸ confirm that the best description of the bonding is that of a true metallaoxirane rather than a π-bonded carbonyl group, in contrast to our earlier observations with Ir stabilized phenoxonium cations.³⁸ The character of the C(*ipso*)-O bond (C1 – O4) is that of a single bond at 1.341(2) Å while the C(*para*)-O bond retains clear double bond character with a 1.251(2) Å (C5 – O1) bond length. The Fe1 – C1 distance is 2.111(9) Å, only slightly longer than in complexes **2**, **4** and **5**. The bond lengths in the ring alternate from double bonds for C3 – C4 (1.359(2) Å) to single bonds for C1 – C3 (1.458(2) Å) and C4 – C5 (1.459(2) Å). The C1 – O4 bond is 16.6° above – and the C1 – Fe1 bond 55.6° below the pincer ring plane, giving C1 the resemblance of a spiro-junction of the six-membered and the three membered rings (Figure 6).

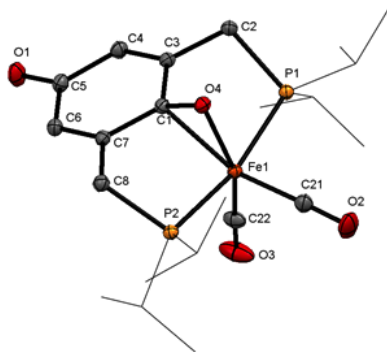


Figure 6. Solid state structure of **6** (thermal ellipsoids set at 50% probability level; isopropyl groups presented as wireframe and hydrogens omitted for clarity). Selected bond lengths [Å] and bond and torsion angles [°] for **6**: Fe1 – C21 1.780(1), Fe1 – C22 1.764(1), Fe1 – C1 2.1111(9), Fe1 – O4 1.9707(8), Fe1 – P1 2.2633(4), Fe1 – P2 2.2676(4), C1 – O4 1.341(2), C5 – O1 1.251(2), C1 – C3 1.458(2), C3 – C4 1.359(2), C4 – C5 1.459 (2), P1 – Fe1 – P2 166.23(1), C1 – Fe1 – C21 147.80(5), Fe1 – C1 – O4 65.25(5), C3 – C1 – O4 119.39(9), C1 – Fe1 – O4 38.15(4), C1 – O4 – Fe1 76.60(6), C22 – Fe1 – C21 96.08(6), C1 – Fe1 – C22 116.11(5), C4 – C3 – C1 – O4 -163.4(1), C4 – C3 – C1 – Fe1 124.4(1).

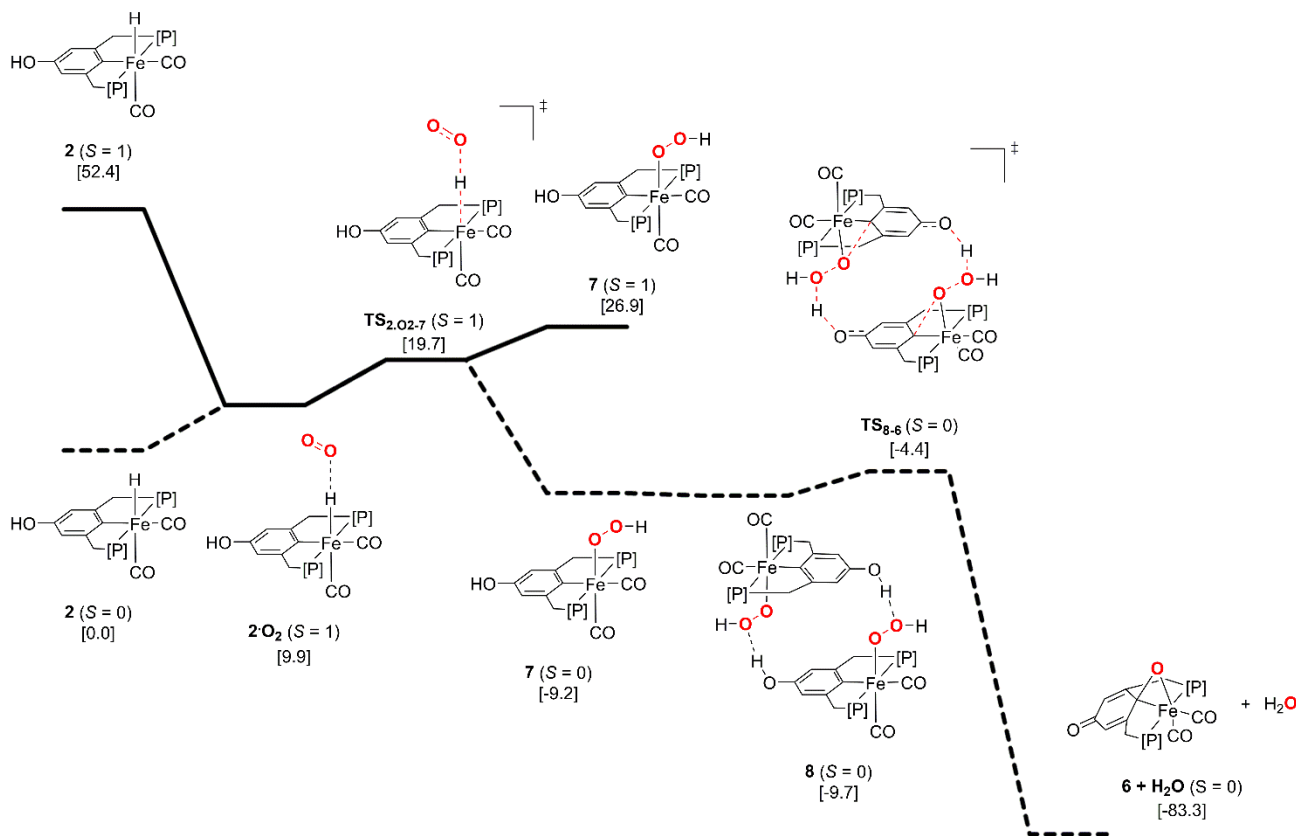


Figure 7. Free energy pathways of oxygen insertion into **2**, calculated at the TPSS-D3BJ/def2-TZVPP//BP86-D3/def2-SV(P) level of theory. Solvent effects are implicit taken into account by using the SMD model. All free energies are given with respect to **2** and $^3\text{O}_2$ (and **7** in the case of **8** and TS_{8-6}).

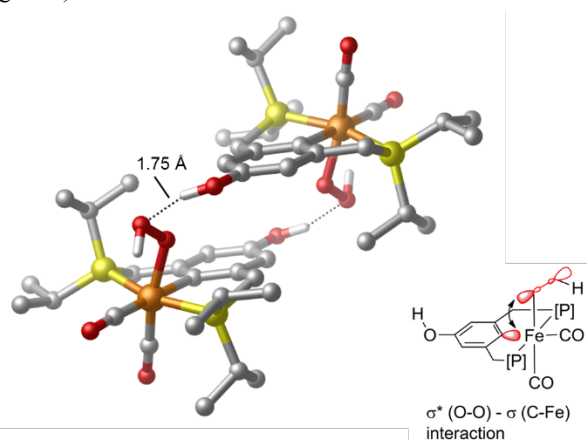
The experimental observation that a full equivalent of oxygen is necessary for the reaction to proceed to completion

A recent report from our group describes the activation of dioxygen by metal-ligand cooperation involving the pincer sidearms of a pyridine-based PNP-Iridium complex.⁴⁷ Likewise, Goldberg^{48,49} and more recently Piers⁵⁰ reported the formation of complexes in which an oxygen atom originating from O_2 or N_2O , respectively is bridging the metal center and the ligand in a fashion similar to that observed in **7**. However, we are not aware of a reported observed O_2 activation process involving O insertion into a metal-aryl bond.⁵¹

The mechanism of the activation of dioxygen by **2** was investigated by DFT calculations at the SMD(THF)-TPSS-D3BJ/def2-TZVPP//BP86-D3/def2-SV(P) level of theory. Initial insertion of O_2 via the long range adduct $2\cdot\text{O}_2$ and $\text{TS}_{2\cdot\text{O}_2-7}$ into the Fe-hydride yields the hydroperoxo complex **7** (Figure 7). A double cross-over pathway for this insertion can be found with a barrier of 19.7 kcal/mol, which would allow this step to occur at room temperature. Exergonic dimerization of **7** leads to the C_i symmetric dimer **8**. Protonation of the hydroperoxy ligand by the hydroxyl group of the second molecule and concomitant C(ipso)-oxygen bond formation yields the oxaferraquinone **6** and one equivalent water as byproduct in an overall strongly exergonic reaction.

supports the proposed mechanism. Essential for the reaction is the formation of the interesting dimeric structure **8**. The DFT

1 optimized structure reveals intermolecular short hydrogen
 2 bonds between the para-hydroxyl group and the hydroperoxy
 3 ligand bound to the iron center of a second molecule (Figure
 4 8). An analysis of the potential energy density at the bond
 5 critical point of these hydrogen bonds revealed that each single
 6 hydrogen bond stabilizes the dimer 8 by -12.9 kcal/mol.
 7 These hydrogen bonds facilitate the protonation and weaken
 8 the O-O bond. Furthermore, the orientation of the hydroperoxy
 9 ligand in 8 allows for an interaction of the Fe-C(ipso) σ -bond
 10 with the antibonding O-O σ^* -bond of the hydroperoxy ligand,
 11 necessary for the SN2-like C-O bond formation to occur
 12 (Figure 8).



13
14
15
16
17
18
19
20
21
22
23
24
25
26
27 **Figure 8.** DFT optimized structure of 8 with a schematic representation of the Fe-C(ipso) σ -bond - O-O σ^* -bond interaction. The computed O--HO hydrogen bond length is shown.

28
29
30
31 In summary, we have developed a conceptually new metal-
 32 ligand cooperation pathway through an unprecedented ferra-
 33 quinone – ferrahydroquinone couple. The metal center shows
 34 cooperativity with three different positions of the ligand in a
 35 formal 1,2 and 1,6 fashion depending on the reaction con-
 36 ditions, which leads to a number of unique reactivity patterns.
 37 The ferraquinone reacts with alcohols to form aldehydes and
 38 lactones, thereby regenerating the ferrahydroquinone. In an
 39 unprecedented reaction for any metal complex, and analogous
 40 to reactions of organic quinones, it activates Br_2 and selectively
 41 incorporates it into the complex. The ferraquinone can be
 42 transferred to its hydrogenated form, the ferrahydroquinone by
 43 activation of molecular hydrogen or alcohols. This compound
 44 instantaneously selectively activates molecular oxygen at
 45 room temperature by metal-ligand cooperation resulting in O-
 46 insertion into the aryl-Fe bond and formation of the corre-
 47 sponding oxyferraquinone. This novel mode of metal-ligand
 48 cooperation harnesses the reactivity of metal center and the
 49 ligand in three different positions alike and the described
 50 diversity in transformations and reactivity modes promises
 51 further fruitful studies with this motif.

52 Experimental Details

53 *General specifications.* All reactions were performed under
 54 a nitrogen atmosphere in a Vacuum Atmospheres Co. Model
 55 Nexus glovebox or using standard Schlenk techniques unless
 56 otherwise noted. All solvents were reagent grade or better.
 57 THF, diethyl ether, benzene, and pentane were refluxed over
 58 sodium and distilled under a nitrogen atmosphere and stored

over activated 3\AA molecular sieves. Dichloromethane was
 dried and stored over activated 3\AA molecular sieves. All
 commercially available reagents were used as received. UVB
 (280-315 nm) irradiation was performed in a Luzchem LZC-
 ORG photoreactor equipped with 10 lamps operated at 60Hz
 (3A, 220V). The vessels used during irradiation were regular
 Pyrex glass Schlenk flasks. Experiments with quartz glass
 vessels yielded the same results and reaction times. NMR
 spectra were recorded using Bruker Avance III 300, Avance
 III 400, and Avance 500 spectrometers at 298K. Chemical
 shifts were referenced to the residual solvent peaks (^1H , ^{13}C),
 as well as to an external standard of phosphoric acid (85%
 solution in D_2O) at 0.0 ppm (^{31}P). Chemical shifts are reported
 in parts per million, and coupling constants (J) are reported in
 hertz. NMR assignments were assisted by ^1H - ^1H -COSY,
 ^1H - ^1H -NOESY, ^1H - ^{13}C -HSQC and ^1H - ^{13}C -HMBC. In the
 ^{13}C -DEPTQ NMR spectra, primary and tertiary carbon signals
 are phased down (d), secondary and quaternary carbon signals
 are phased up (u). IR spectra were recorded on a Thermo
 Scientific Nicolet 6700 FT-IR spectrophotometer as thin films
 on NaCl or CaF_2 disks. Electrospray ionization mass spec-
 trometry (ESIMS) spectra were recorded on a Micromass ZQ
 V4.1 by the Chemical Research Support Unit of the Weiz-
 mann Institute of Science. Crystal data for complexes 4,5 and
 6 were measured at 100 K on a Bruker Kappa Apex-II CCD
 diffractometer equipped with [$\lambda(\text{Mo K}\alpha) = 0.71073\text{\AA}$] radi-
 ation, a graphite monochromator, and MiraCol optics. The data
 were processed with APEX2 collect package programs. Struc-
 tures were solved by the AUTOSTRUCTURE module and
 refined with full-matrix least squares refinement based on F2
 with SHELXL-2013.

Data for complex 2 was collected on APEX2 and then in the
 synchrotron ESRF ID-29. Data were processed with HKL2000
 keeping the Friedel Pairs separate. The structure was solved
 with SHELXT. The best suggested solution was a non-
 centrosymmetric space group Pc with 12 molecules in the
 asymmetric unit cell and Flack parameter 0.49 and most of the
 iso-propyl side chains were missing. Data was processed again
 with CrysAlisPro keeping the FP separate and the initial solu-
 tion with SHELXT contained almost all the atoms (including
 iso-propyl side chains). The structure was further refined with
 SHELXL-2013 with full-matrix least squares refinement based
 on F2. The refinement was extremely complex due to the high
 level of the molecules disorder and twinning. Many constraints
 were applied in order to bring the refinement to completion.
 The hydride was calculated and placed at 1.5\AA from the metal
 center in direct extension of the Fe-CO bond.

59
60
Synthesis of 1. Method A: In a 5 mL vial equipped with a
 Teflon stirbar was placed 2 (10 mg, 0.021 mmol) in dry ben-
 zene (1 mL) and stirred. A solution of benzoquinone (4.5 mg,
 0.042 mmol) was added and the reaction mixture turned from
 yellow to deep orange-brown. The mixture was stirred for 30
 min. at room temperature and then filtered and the solvent was
 removed in vacuo. The crude residue was extracted with pen-
 tane (5×0.5 mL) and the extracts combined and dried to give a
 dark orange powder (8 mg, 0.018 mmol, 86%). *Method B:* In a
 20 mL scintillation vial equipped with a Teflon stirbar was
 placed 4 (150 mg, 0.300 mmol) in dry benzene (6 mL) and
 stirred. A solution of KHMDS (72 mg, 0.360 mmol) was
 added dropwise and the reaction mixture turned from yellow
 to deep orange-brown with some precipitate forming. The
 mixture was stirred for 30 min. at room temperature and then
 filtered and the solvent was removed *in vacuo*. The crude was

1 extracted with pentane (5x3 mL) and the extracts pooled and
 2 dried to give a dark orange powder (83 mg, 0.179 mmol,
 3 60%). ¹H NMR (300 MHz, C₆D₆) δ ppm 6.87 (s, 2H, *Ar*), 3.77-
 4 3.10 (m, 4H, *Ar-CH₂-P*), 2.44 (br. s., 2H, *CH_{iPr}*), 2.07 (br. s.,
 5 2H, *CH_{iPr}*), 1.61-0.62 (m, 24H, *iPr*). ¹³C{¹H} NMR (126
 6 MHz, C₆D₆) δ ppm 217.8(u) (t, *J_{C-P}*=27.5 Hz, *CO*), 214.8(u) (t,
 7 *J_{C-P}*=11.8 Hz, *CO*), 170.1(u) (s, *C=O*), 148.4(u) (s, *Ar*),
 8 117.1(d) (br. s., *Ar*), 37.2.4(u) (br. s., *Ar-CH₂-P*), 26.5(d) (t, *J_{C-P}*
 9 *P*=7.6 Hz, *CH_{iPr}*), 25.2(d) (t, *J_{C-P}*=25.1 Hz, *CH_{iPr}*), 19.9(d) (s,
 10 *iPr*), 19.8(d) (s, *iPr*), 19.5(d) (s, *iPr*), 19.4(d) (s, *iPr*). ³¹P{¹H}
 11 NMR (121 MHz, C₆D₆) δ ppm 94.5. IR 1983, 1921, 1563 cm⁻¹.
 12 HRMS (ESI) calc. 465.1411 (C₂₂H₃₄O₃P₂Fe + H⁺), found
 13 465.1409.

14 **Synthesis of 2.** In a 100 mL Schlenk flask equipped with a
 15 Teflon stirbar was placed **3** (400 mg, 1.13 mmol) in dry THF
 16 (15 mL). Fe(CO)₅ (200 mg, 1.02 mmol) was added, the flask
 17 was sealed and put in a UVB reactor with stirring at room
 18 temperature. CO gas forming in the course of the reaction was
 19 vented after 6 h and again after 18 h and 48 h. After 4 days the
 20 reaction mixture was emerald green and the volatiles were
 21 removed *in vacuo*. The residue was washed with pentane (3 x
 22 5 mL) and dried to yield **2** as a green powder (390 mg, 0.837
 23 mmol, 82%). Crystals (fine needles) suitable for X-ray analy-
 24 sis were obtained by slow diffusion of pentane into a solution
 25 of **2** in Et₂O/pentane (1:1). ¹H NMR (300 MHz, C₆D₆) δ ppm
 26 6.48 (s, 2H, *Ar*), 3.86 (br. s., 1H, *ArOH*), 3.15-2.93 (m, 2H,
 27 *Ar-CH₂-P*), 2.79 (dt, *J*=16.48, 4.58 Hz, 2H, *Ar-CH₂-P*), 2.10-
 28 1.74 (m, 4H, *CH_{iPr}*) 1.32-0.98 (m, 18H, *iPr*), 0.92-0.76 (m,
 29 6H, *iPr*) -8.81 (t, *J_{H-P}*=50.4 Hz, 1H, Fe-H). ¹³C{¹H} NMR,
 30 DEPT-Q (126 MHz, C₆D₆) δ ppm 217.2(u) (t, *J*=15.5 Hz,
 31 *CO*), 216.5(u) (t, *J*=12.0 Hz, *CO*), 159.3(u) (t, *J_{C-P}*=13.4 Hz,
 32 *ArC-Fe*), 153.6(u) (s, *ArC-OH*), 147.1(u) (t, *J_{C-P}*=10.2 Hz, *Ar*),
 33 109.9(d) (s, *Ar*), 39.4(u) (t, *J_{C-P}*=13.6 Hz, *Ar-CH₂-P*), 28.4(d)
 34 (t, *J_{C-P}*=9.2 Hz, *CH_{iPr}*), 26.9(d) (t, *J_{C-P}*=14.3 Hz, *CH_{iPr}*),
 35 18.9(d) (s, *iPr*), 18.7(d) (s, *iPr*), 18.5(d) (s, *iPr*), 18.1(d) (s,
 36 *iPr*). ³¹P{¹H} NMR (121 MHz, C₆D₆) δ ppm 111.5 (s) IR
 37 1967, 1920, 1888 (Fe-H), 1590 cm⁻¹. Elemental Analysis,
 38 Calc'd for C₂₂H₃₆FeO₃P₂: C, 56.67; H, 7.78; Fe, 11.98; O,
 39 10.29; P, 13.28. Found: C, 56.46; H, 8.26

40 **Synthesis of 3.** Di(bromomethyl)phenol was prepared ac-
 41 cording to a literature procedure.¹⁴ In a thick walled 250 mL
 42 round-bottom flask equipped with a Teflon stirbar was placed
 43 a solution of the dibromide (2.82 g, 10 mmol) and di(isopropyl)phosphine
 44 (5.88 g, 50 mmol) in methanol (30 mL). The flask was sealed with a
 45 Teflon screwcap and the clear, amber solution was heated to 50°C with
 46 stirring for 2 days. Triethylamine (8.3 mL, 60 mmol) was added under
 47 inert atmosphere and the resulting solution was stirred for 30 min.
 48 at room temperature. The volatiles were removed *in vacuo* and
 49 the residue was taken up repeatedly in diethylether and the
 50 volatiles were removed again *in vacuo* (4 x 20 mL). The ligand
 51 was crystallized from a cooled and highly concentrated
 52 pentane solution to give colorless crystals (2.93 g, 8.26 mmol,
 53 83%). ¹H NMR (300 MHz, C₆D₆) δ ppm 6.96 (s, 1H, *Ar*), 6.67
 54 (s, 2H, *Ar*), 4.80 (br. s., 1H, *ArOH*), 2.63 (s, 4H, *Ar-CH₂-P*),
 55 1.60 (h, 4H, *CH_{iPr}*), 0.99 (m, 24H, *iPr*). ³¹P{¹H} NMR (121
 56 MHz, C₆D₆) δ ppm 9.5 (s).

57 **Synthesis of 4.** In a 20 mL scintillation vial equipped with a
 58 Teflon stirbar was placed **2** (100 mg, 0.215 mmol) in dry
 59 benzene (5 mL), sealed with a septum screw-cap and stirred.
 60 Concentrated aqueous HCl (50 μL, 0.54 mmol) was added
 dropwise and the reaction mixture turned from green to yellow

with some gas evolution. The mixture was stirred for 1 hr at
 room temperature and the volatiles were removed *in vacuo*.
 The crude was extracted with THF (3 x 2 mL) and the filtered
 extracts combined and dried to give **4** as a light yellow powder
 (93 mg, 0.186 mmol, 87%). ¹H NMR (400 MHz, CDCl₃) δ
 ppm 6.63 (s, 2 H, *Ar*), 4.47 (br. s., 1 H, *ArOH*), 3.57 (dt,
J=15.6, 4.6 Hz, 2H, *Ar-CH₂-P*), 3.33 (dt, *J*=15.6, 3.7 Hz, 2H,
Ar-CH₂-P), 3.03-2.89 (m, 2H, *CH_{iPr}*), 2.51-2.35 (m, 2H,
CH_{iPr}), 1.45-1.32 (m, 12H, *iPr*) 1.30-1.20 (m, 12H, *iPr*).
¹³C{¹H} NMR, DEPT-Q (100.7 MHz, CDCl₃) δ ppm 216.1(u)
 (t, *J_{C-P}*=25.6 Hz, *CO*), 212.1(u) (t, *J_{C-P}*=13.6 Hz, *CO*), 160.0(u)
 (t, *J_{C-P}*=12.8 Hz, *ArC-Fe*), 154.2(u) (s, *ArC-OH*), 148.3(u) (t,
J_{C-P}=8.5 Hz, *Ar*) 110.9(d) (t, *J_{C-P}*=7.4 Hz, *Ar*), 37.7(u) (t, *J_{C-P}*
P=15.0 Hz, *Ar-CH₂-P*), 26.1(d) (t, *J_{C-P}*=9.9 Hz, *CH_{iPr}*) 24.9 (t,
J_{C-P}=9.9 Hz, *CH_{iPr}*), 19.7(d) (s, *iPr*), 19.6(d) (s, *iPr*), 19.5(d)
 (s, *iPr*), 19.3(d) (s, *iPr*). ³¹P{¹H} NMR (162.1 MHz, CDCl₃) δ
 ppm 94.1 (s). IR 1995, 1932 cm⁻¹.

Synthesis of 5. In a 20 mL scintillation vial equipped with a
 Teflon stirbar was placed **1** (20 mg, 0.043 mmol) in dry ben-
 zene (3 mL), sealed with a septum screw-cap and stirred. A
 solution of Br₂ in dry benzene (1 wt%, 0.5 mL, 0.097 mmol)
 was added dropwise and the reaction mixture turned from dark
 brown-orange to a vibrant bright orange. The mixture was
 stirred for 1 hr at room temperature, filtered and the volatiles
 were removed *in vacuo*. The crude was extracted with a mix-
 ture of pentane/Et₂O (1:1, 3 x 2 mL) and the filtered extracts
 were combined and dried to give **5** as a bright orange powder
 (28 mg, 0.040 mmol, 93%). Crystals (prisms) suitable for X-
 ray analysis were obtained by slow diffusion of pentane into a
 solution of **5** in Et₂O/pentane (1:1). ¹H NMR (400 MHz, C₆D₆)
 δ ppm 5.60 (br. s., 1H, *PhOH*), 3.89 (dt, *J*=16.5, 4.3 Hz, 2H,
Ar-CH₂-P), 3.48 (dt, *J*=16.5, 3.6 Hz, 2H, *Ar-CH₂-P*), 3.12-2.99
 (m, 2H, *CH_{iPr}*), 2.02-1.89 (m, 2H, *CH_{iPr}*), 1.22-1.09 (m, 6H,
iPr) 1.07-0.85 (m, 18H, *iPr*). ¹³C NMR, DEPT-Q (100.7 MHz,
 C₆D₆) δ ppm 217.5(u) (t, *J_{C-P}*=25.7 Hz, *CO*), 212.7(u) (t, *J_{C-P}*
P=14.5 Hz, *CO*), 160.5(u) (t, *J_{C-P}*=13.6, *ArC-Fe*), 147.1(u) (s,
ArC-OH), 146.2(u) (t, *J_{C-P}*=8.2 Hz, *Ar*) 107.4(u) (t, *J_{C-P}*=7.0
 Hz, *Ar*), 40.8(u) (t, *J_{C-P}*=15.8 Hz, *Ar-CH₂-P*), 26.5(d) (t, *J_{C-P}*
P=10.7 Hz, *CH_{iPr}*), 26.4(d) (t, *J_{C-P}*=9.8 Hz, *CH_{iPr}*), 19.4(d) (s,
iPr), 19.3(d) (s, *iPr*), 19.1(d) (s, *iPr*), 19.0(d) (s, *iPr*). ³¹P
 NMR (162.1 MHz, C₆D₆) δ ppm 84.7 (s). IR 2003, 1941 cm⁻¹.
 LRMS (ESI) 724.89 (highest abundance peak, 1:3:3:1 isotope
 pattern for 3 Br) (C₂₂H₃₃Br₃O₃P₂Fe + Na⁺).

Synthesis of 6. In a 20 mL scintillation vial equipped with a
 Teflon stirbar was placed **2** (60 mg, 0.129 mmol) in dry ben-
 zene (5 mL). The vial was removed from the glovebox and a
 stream of O₂ was bubbled through the solution for 10 sec. The
 dark mixture was filtered, yielding a black filter residue and a
 bright orange filtrate. The volatiles of the filtrate were re-
 moved *in vacuo* to give **6** as a bright orange powder (32 mg,
 0.067 mmol, 52%). Crystals (prisms) suitable for X-ray analy-
 sis were obtained by slow diffusion of pentane into a solution
 of **5** in toluene.

To test the stoichiometry of the reaction, the reaction was
 repeated under identical conditions with the addition of only
 0.5 equiv. and 1 equiv. of O₂, respectively, added via a gas-
 tight syringe through a septum. The work-up was performed in
 an analogous fashion inside the glovebox and it was found that
 in the case of the addition of only 0.5 equiv. of O₂ that the
 conversion of the starting material was not complete. In con-
 trast, in the case of addition of one full equivalent of O₂, the
 starting material had been fully consumed. ¹H NMR (400

1
2
3
4
5
6
7
8
9
10
11
12
13
14
15
16
17
18
19
20
21
22
23
24
25
26
27
28
29
30
31
32
33
34
35
36
37
38
39
40
41
42
43
44
45
46
47
48
49
50
51
52
53
54
55
56
57
58
59
60

MHz, C₆D₆) δ ppm 6.53 (s, 2H, Ar), 2.58-2.38 (m, 2H, Ar-CH₂-P), 1.89-1.73 (m, 2H, CH_(iPr)), 1.72-1.53 (m, 2H, CH_(iPr)), 1.44 - 1.24 (m, 6 H, iPr), 1.19-0.75 (m, 14H, Ar-CH₂-P and iPr), 0.74-0.59 (m, 6 H, iPr). Residual toluene at 2.1 ppm ¹³C{¹H} NMR, DEPT-Q (100.7 MHz, C₆D₆) δ ppm 217.0(u) (t, J=21.1 Hz, CO), 215.60(u) (t, J=22.7 Hz, CO) 183.6(u) (s, ArC=O), 157.4(u) (s, Ar), 124.6(d) (t, J=5.1 Hz, Ar), 96.7(u) (t, J=2.2 Hz, ArC-Fe), 26.4(d) (t, J=10.2 Hz, CH_(iPr)), 20.2(u) (t, J=9.6 Hz, Ar-CH₂-P), 17.9(d) (s, iPr), 17.4(d) (s, iPr), 17.0(d) (s, iPr), 16.7(d) (s, iPr). ³¹P{¹H} NMR (162.1 MHz, C₆D₆) δ ppm 69.4 (s). IR 1967, 1904 cm⁻¹. LRMS (ESI) 503.19 (C₂₂H₃₄O₄P₂Fe + Na⁺). Elemental Analysis, Calc'd for C₂₂H₃₄FeO₄P₂: C, 55.02; H, 7.14; Fe, 11.63; O, 13.32; P, 12.90. Found: C, 54.47; H, 7.62

Computational details. All geometries were optimized with the BP86 generalized-gradient approximation (GGA) functional and the def2-SV(P) basis set together with corresponding core potential for ruthenium. The D3 dispersion correction was used for the geometry optimizations. Thermodynamic properties were obtained at the same level of theory from a frequency calculation. All free energies are calculated under standard conditions unless otherwise noted. Minima and transition states were characterized by the absence and presence of one imaginary frequency, respectively. For a comparison with the experimentally observed IR-spectra the structures of **1**, **2**, **4** and **6** were reoptimized at the same level of theory with the larger def2-TZVP basis set. Single point calculations were obtained with the TPSS meta-GGA functional in combination with the D3 dispersion correction and Becke-Johnson damping and the larger triple-zeta plus polarization def2-TZVPP basis set. The TPSS functional was recently shown to yield results very close to explicitly correlated coupled cluster benchmark calculations for reaction energies and barriers involving transition metal complexes with pincer ligands. In order to improve the computational efficient, the density fitting approximation with the W06 fitting basis sets, designed for use with the def2 basis sets, was used. In order to take solvent effects into account, the SMD solvation model for THF was used for the single point calculations. The "ultrafine" (i.e., a pruned (99,590)) grid was used for all calculations. All calculations were performed using Gaussian 09 Revision D.01.

ASSOCIATED CONTENT

Supporting Information containing experimental details of synthetic procedures, X-ray data and computational details. This material is available free of charge via the Internet at <http://pubs.acs.org>.

AUTHOR INFORMATION

Corresponding Author

* david.milstein@weizmann.ac.il

Author Contributions

δ These authors contributed equally

The manuscript was written through contributions of all authors. / All authors have given approval to the final version of the manuscript. /

ACKNOWLEDGMENT

This research was supported by the European Research Council (ERC AdG 692775) and by the Kimmel Center for Molecular Design. AD thanks the Austrian Science Fund for an Erwin Schrodinger Postdoctoral Fellowship and the Azrieli Foundation for a Research and Materials Grant. UG thanks the DAAD for a Post Doctoral Fellowship and the Feinberg Graduate School for a Senior Post-Doctoral Award. DM holds the Israel Matz Professorial Chair of Organic Chemistry. We thank Linda J. W. Shimon for collecting data in the ERSF ID-29 and the staff members of ERSF ID-29 are acknowledged for their support.

REFERENCES

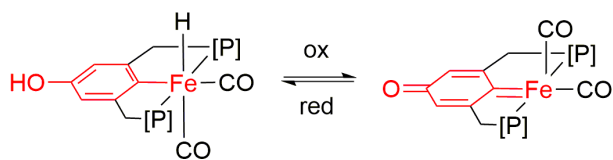
- (1) The Chemistry of the Quinoid Compounds, Parts 1 and 2 (Ed.: S. Patai). Wiley, London, **1974**; The Chemistry of the Quinoid Compounds, Parts 1 and 2 (Eds.: S. Patai, Z. Rappoport). Wiley, Chichester, **1988**.
- (2) Campos-Martin, J. M.; Blanco-Brieva, G.; Fierro, J. L. G. *Angew. Chem. Int. Ed.* **2006**, *45*, 6962–6984.
- (3) Abraham, I.; Joshi, R.; Pardasani, P.; Pardasani, R. *J. Braz. Chem. Soc.* **2011**, *22*, 385–421.
- (4) Bäckvall, J.-E.; Hopkins, R. B.; Grennberg, H.; Mader, M.; Awasthi, A. K. *J. Am. Chem. Soc.* **1990**, *112*, 5160–5166; Piera, J.; Bäckvall, J.-E. *Angew. Chem. Int. Ed.* **2008**, *47*, 3506–3523.
- (5) Zhang, Y.; Li, C.-J. *J. Am. Chem. Soc.* **2006**, *128*, 4242–4243.
- (6) Guo, X.; Zipse, H.; Mayr, H. *J. Am. Chem. Soc.* **2014**, *136*, 13863–13873.
- (7) Lerch, S.; Unkel, L.-N.; Brasholz, M. *Angew. Chem. Int. Ed.* **2014**, *53* (25), 6558–6562.
- (8) Brasholz, M.; Lerch, S.; Unkel, L.-N.; Wienefeld, P. *Synlett* **2014**, *25*, 2673–2680.
- (9) Zhou, L.; Xu, B.; Zhang, J. *Angew. Chem. Int. Ed.* **2015**, *54*, 9092–9096.
- (10) Ernster, L.; Dallner, G. *Biochim. Biophys. Acta - Mol. Basis Dis.* **1995**, *1271*, 195–204.
- (11) Ernster, L.; Forsmark-Andrée, P. *Clin. Investig.* **1993**, *71*, 60–65.
- (12) Milton, R. D.; Hickey, D. P.; Abdellaoui, S.; Lim, K.; Wu, F.; Tan, B.; Minter, S. D. *Chem. Sci.* **2015**, *6*, 4867–4875.
- (13) Bauer, I.; Knölker, H.-J. *Chem. Rev.* **2015**, *115*, 3170–3387.
- (14) Bolm, C.; Legros, J.; Paih, J. L.; Zani, L. *Chem. Rev.* **2004**, *104*, 6217–6254.
- (15) Enthaler, S.; Junge, K.; Beller, M. *Angew. Chem. Int. Ed.* **2008**, *47*, 3317–3321.
- (16) Langer, R.; Leitius, G.; Ben-David, Y.; Milstein, D. *Angew. Chem. Int. Ed.* **2011**, *50*, 2120–2124.
- (17) Langer, R.; Diskin-Posner, Y.; Leitius, G.; Shimon, L. J. W.; Ben-David, Y.; Milstein, D. *Angew. Chem. Int. Ed.* **2011**, *50*, 9948–9952.
- (18) Langer, R.; Iron, M. A.; Konstantinovski, L.; Diskin-Posner, Y.; Leitius, G.; Ben-David, Y.; Milstein, D. *Chem. Eur. J.* **2012**, *18*, 7196–7209.
- (19) Zell, T.; Butschke, B.; Ben-David, Y.; Milstein, D. *Chem. Eur. J.* **2013**, *19*, 8068–8072.
- (20) Srimani, D.; Diskin-Posner, Y.; Ben-David, Y.; Milstein, D. *Angew. Chem. Int. Ed.* **2013**, *52*, 14131–14134.
- (21) Rivada-Wheelaghan, O.; Dauth, A.; Leitius, G.; Diskin-Posner, Y.; Milstein, D. *Inorg. Chem.* **2015**, *54* (9), 4526–4538.
- (22) Butschke, B.; Fillman, K. L.; Bendikov, T.; Shimon, L. J. W.; Diskin-Posner, Y.; Leitius, G.; Gorelsky, S. I.; Neidig, M. L.; Milstein, D. *Inorg. Chem.* **2015**, *54*, 4909–4926.
- (23) Zell, T.; Milstein, D. *Acc. Chem. Res.* **2015**, *48* (7), 1979–1994.
- (24) Garg, J. A.; Chakraborty, S.; Ben-David, Y.; Milstein, D. *Chem. Commun.* **2016**, *52*, 5285–5288.

- (25) Rivada-Wheelaghan, O.; Chakraborty, S.; Shimon, L. J. W.; Ben-David, Y.; Milstein, D. *Angew. Chem. Int. Ed.* **2016**, *55*, 6942–6945.
- (26) Ashkenazi, N.; Vigalok, A.; Parthiban, S.; Ben-David, Y.; Shimon, L. J. W.; Martin, J. M. L.; Milstein, D. *J. Am. Chem. Soc.* **2000**, *122*, 8797–8798.
- (27) Vigalok, A.; Rybtchinski, B.; Gozin, Y.; Koblenz, T. S.; Ben-David, Y.; Rozenberg, H.; Milstein, D. *J. Am. Chem. Soc.* **2003**, *125*, 15692–15693.
- (28) Vigalok, A.; Milstein, D. *Acc. Chem. Res.* **2001**, *34*, 798–807.
- (29) a) Vigalok, A.; Milstein, D. *J. Am. Chem. Soc.* **1997**, *119*, 7873–7874; b) Poverenov, E.; Milstein, D. Quinone methide stabilization by metal complexation. in “Quinone Methides” S, Rokita, Ed, Wiley, **2009**, 69–88 (2009).
- (30) Kharisov, B.; Méndez-Rojas, M.; Garnovskii, A.; Ivakhnenko, E.; Ortiz-Méndez, U. *J. Coord. Chem.* **2002**, *55*, 745–770.
- (31) Kim, S. B.; Pike, R. D.; Sweigart, D. A. *Accounts of Chemical Research Acc. Chem. Res.* **2013**, *46*, 2485–2497.
- (32) a) Moussa, J.; Amouri, H. *Angew. Chem. Int. Ed.* **2008**, *47*, 1372–1380; b) Moussa, J.; Lev, D. A.; Bouberkeur, K.; Rager, M. N.; Amouri, H. *Angew. Chem. Int. Ed.* **2006**, *45*, 3854–3858 c) Amouri, H.; Moussa, J.; Renfrew, A. K.; Dyson, P. J.; Rager, M. N.; Chamoireau, L.-M. *Angew. Chem. Int. Ed.* **2010**, *49*, 7530–7533; d) Amouri, H.; Le Bras, J. *Acc. Chem. Res.* **2002**, *35*, 501–510; e) Moussa, J.; Guyard-Duhayon, C.; Herson, P.; Amouri, H. *Organometallics* **2004**, *23*, 6231–6238.
- (33) Mitsumi, M.; Ezaki, K.; Komatsu, Y.; Toriumi, K.; Miyatou, T.; Mizuno, M.; Azuma, N.; Miyazaki, Y.; Nakano, M.; Kitagawa, Y.; Hanashima, T.; Kiyonagi, R.; Ohhara, T.; Nakasuji, K. *Chem. Eur. J.* **2015**, *21*, 9682–9696.
- (34) Zhang, S.-S.; Jiang, C.-Y.; Wu, J.-Q.; Liu, X.-G.; Li, Q.; Huang, Z.-S.; Li, D.; Wang, H. *Chem. Commun.* **2015**, *51*, 10240–10243.
- (35) Horak, K. T.; Agapie, T. *J. Am. Chem. Soc.* **2016**, *138*, 3443–3452
- (36) Review: Khusnutdinova, J. R.; Milstein, D. *Angew. Chem. Int. Ed.* **2015**, *54*, 12236–12273.
- (37) Grützmacher, H. *Angew. Chem. Int. Ed.* **2008**, *47*, 1814–1818.
- (38) Vlugt, J. I. V. D. *Eur. J. Inorg. Chem.* **2012**, *3*, 363–375.
- (39) Ikariya, T. *Top. Organomet. Chem.* **2011**, 31–53.
- (40) Gunanathan, C.; Milstein, D. *Acc. Chem. Res.* **2011**, *44*, 588–602.
- (41) Due to the extreme air-sensitivity of the crystals, the resulting data was often insufficient for full refinement. It was found serendipitously that exposing the crystals to air for an extended period of time resulted in better diffraction data. This was attributed to the likely formation of a protective but non-diffracting oxide layer on the surface of the crystal.
- (42) Bhattacharya, P.; Krause, J. A.; Guan, H. *Organometallics* **2011**, *30*, 4720–4729.
- (43) Sanctis, D. D.; Beteva, A.; Caserotto, H.; Dobias, F.; Gabadinho, J.; Giraud, T.; Gobbo, A.; Guijarro, M.; Lentini, M.; Lavault, B.; Mairs, T.; Mcsweeney, S.; Petitdemange, S.; Rey-Bakaikoa, V.; Surr, J.; Theveneau, P.; Leonard, G. A.; Mueller-Dieckmann, C. *J. Synchrotron Rad.* **2012**, *19*, 455–461.
- (44) Complexes in which a metal-coordinated carbene cannot be detected by ^{13}C NMR were reported: a) Alcarazo, M.; Roseblade, S. J.; Cowley, A. R.; Fernández, R.; Brown, J. M.; Lassaletta, J. M. *J. Am. Chem. Soc.* **2005**, *127*, 3290–3291. b) Mayr, M.; Wurst, K.; Ongania, K.-H.; Buchmeiser, M. R. *Chem. Eur. J.* **2004**, *10* (5), 1256–1266. c) Coleman, K. S.; Chamberlayne, H. T.; Turberville, S.; Green, M. L. H.; Cowley, A. R. *Dalton Trans.* **2003**, *14*, 2917–2922.
- (45) For full computational details and calculations see Supplementary Information.
- (46) When the compound was heated to a melt under vacuum, a complex product mixture was formed which, according to FT-IR spectroscopy, contained 1 but was NMR silent and eluded further characterization.
- (47) Feller, M.; Ben-Ari, E.; Diskin-Posner, Y.; Carmieli, R.; Weiner, L.; Milstein, D. *J. Am. Chem. Soc.* **2015**, *137*, 4634–4637.
- (48) Scheuermann, M. L.; Fekl, U.; Kaminsky, W.; Goldberg, K. I. *Organometallics* **2010**, *29*, 4749–4751.
- (49) Scheuermann, M. L.; Luedtke, A. T.; Hanson, S. K.; Fekl, U.; Kaminsky, W.; Goldberg, K. I. *Organometallics* **2013**, *32*, 4752–4758.
- (50) Vitcu, A. *J. Am. Chem. Soc.* **2003**, *137*, 2–4.
- (51) Zhang, Y.-H.; Yu, J.-Q. *J. Am. Chem. Soc.* **2009**, *131*, 14654–14655.

For TOC

ferrahydroquinone (FHQ)

ferraquinone (FQ)



Reactivity towards

O₂, alkynes, acidH₂, alcohols, Br₂, acid